RAPID COMMUNICATIONS

PHYSICAL REVIEW E VOLUME 47, NUMBER 5 MAY 1993

Directed polymers in a random medium: Universal scaling behavior of the probability distribution

Yadin Y. Goldschmidt and Thomas Blum
Department of Physics and Astronomy, University of Pittsburgh, Pittsburgh, Pennsylvania 15260
(Received 4 December 1992)

We study the probability distribution $P(x,t)$ for the head of a directed polymer in a random medium in $1+1$ dimensions. We find that, as a function of the scaling variable $u=|x|/t^{2/3}$, the behavior of the probability distribution changes abruptly at $u_c \approx 1.2$. Its universal part is given by $P \propto \exp(-\alpha u^y)$ where the exponent α is distributed for different samples according to $\mathcal{P}(\alpha)=\mathcal{N}\exp[-f(\alpha)u^y]$. For $0.25 \lesssim u < u_c$, $y=2.1\pm0.1$ and the multifractal measure $f(\alpha)$ is a convex function with a minimum at α_{typ}, which is the exponent associated with a typical sample of the disorder. For $u \gg u_c$, $y=3.0\pm0.1$ and $f(\alpha)$ becomes trivial.

PACS number(s): 05.40.+j, 05.20.−y, 75.10.Nr, 02.50.−r

In the last few years, considerable attention has been focused on the role of disorder and random perturbations in the statics and dynamics of various systems, whether concerning bulk properties or the scaling behavior of rough interfaces. Recently some progress has been made both theoretically [1–9] and experimentally [10] on the problem of directed walks in random media and more generally of directed manifolds [11]. These models share many properties of more notorious disordered systems, such as spin glasses, but are considered "simpler." Furthermore, they are of fundamental interest because of the mapping of such systems to the Kardar-Parisi-Zhang equation for interface growth and to the Burgers equation for randomly stirred fluids [12]. Here we demonstrate that this model can be analyzed using the powerful tool of multifractal formalism introduced previously for dynamical systems [13–20].

A directed walk (or directed polymer) is a path in $d+1$ dimensions, for which one of the coordinates (called "time") is always increasing along the path. One may consider such a walk on a disordered substrate by having it interact with a random potential at each site. In these models, the disorder is "time"-dependent and uncorrelated along that axis. In $1+1$ dimensions, the model may describe a domain wall (without "overhangs") in a disordered Ising model [1]. Some of the properties of directed polymers in random media, such as the wandering exponent $\nu(\langle\langle x^2\rangle_T\rangle_R \sim t^{2\nu})$ and the exponent characterizing the free-energy fluctuations are known exactly in $1+1$ dimensions [2,3], provided the spatial correlations of the disorder are short ranged. One method [2] for extracting these exponents uses a Bethe ansatz for the ground-state wave function of an associated replicated Hamiltonian, and another method [3] uses some known properties of the Burgers equation. The exponent $\nu=\frac{2}{3}$ indicates superdiffusivity, the tendency of the walk to wander farther in the transverse direction (than it would for purely entropic reasons) in order to take advantage of the random potential. While these two exponents are known exactly, the model has many features that are not yet understood. For instance, there is no known exact expression for the Green's function (although some approximate formulas have been suggested within the framework of the replica formulation) [4–6].

In this Rapid Communication we report on some results concerning the probability distribution for the head of a directed polymer in a random medium. We have based these results on extensive numerical simulations together with a theoretical interpretation and analysis. At a finite temperature $1/\beta$, the walker acquires a random Boltzmann factor $e^{-\beta V(x,t)}$ at each site it visits, where $V(x,t)$ satisfies

$$\langle V(x,t)V(x',t')\rangle = v_0\delta(t-t')\delta(x-x') , \tag{1}$$

and where $\langle\ \rangle$ indicates averaging over the random potential. In this work we have used a random potential with a Gaussian distribution, zero mean, and standard deviation of 1. The partition function (or Green's function) is given by

$$Z(x,t)=\sum_{\text{paths }(x',t')\in\text{path}} \prod e^{-\beta V(x',t')} , \tag{2}$$

which sums over all possible directed paths connecting (0,0) to (x,t). The probability distribution is then defined as

$$P(x,t)=\frac{Z(x,t)}{\sum_{x'} Z(x',t)} . \tag{3}$$

Given the scaling of the transverse fluctuations, it is convenient to introduce the variable $u=|x|/t^{2/3}$. We have found that for large t and for $u \lesssim 0.25$ the average probability distribution takes the scaling form $\langle P(x,t)\rangle = t^{-2/3}\hat{P}(u)$. Furthermore, we have observed that $\hat{P}(u)$ changes from

$$\hat{P}(u)\sim\exp\{-\lambda_1 u^2\} \quad \text{for } 0.25 \le u \le 1.2 \tag{4a}$$

to

$$\hat{P}(u)\sim\exp\{-\lambda_2 u^3\} \quad \text{for } 2.0 \le u , \tag{4b}$$

with an unsmooth transition region in between $(1.2 \le u \le 2.0)$.

More generally, one can characterize the behavior of $P(x,t)$ among different realizations of the disorder by a distribution of exponents, provided by a universal function $f(\alpha)$. Such a function is reminiscent of the multifractal spectrum introduced for dynamical systems for describing the distribution of fractal dimensions corresponding to strange attractor sets with different associated singularities [13]. Similar rich scaling behavior has also been found in other complex inhomogeneous sys-

tems, such as turbulence [14], diffusion-limited aggregation (DLA) [15], Anderson localization [16], random-resistor networks [17], and random walks on percolation clusters [18]. Closer in nature to the present application of this formalism are recent studies of scaling in diluted ferromagnets [19] and of flow in stratified media with random velocity fields [20], both involving many realizations of spatial disorder.

In the present case, $f(\alpha)$ governs the distribution of the exponents α in the expression

$$P(x,t)\sim\exp\{-\alpha\lambda u^{y}\} . \tag{5}$$

Notice that P is not averaged and that this expression includes both regions of Eq. (4) where $\lambda=\lambda_1$, $y\approx 2$ in region 1 and $\lambda=\lambda_2$, $y\approx 3$ in region 2. The value corresponding to the minimum of $f(\alpha)$, $\alpha_{\rm typ}$ characterizes the behavior of P for a typical realization; it is larger than $\alpha=1$, which yields the mean behavior. The large parameter in our model, which allows for the extraction of the multifractal behavior (the analog of $1/l$ in dynamical systems [13]), is a combination of t and u [see Eqs. (11) and (12) below].

We now present the results in greater detail. We have evaluated the Green's function $Z(x,t)$ defined in Eq. (2) by using the recursion relation [21]

$$Z(x,t)=[Z(x-1,t-1)+Z(x+1,t-1)]\times\exp\{-\beta V(x,t)\} , \tag{6}$$

with $Z(0,0)=1$. This method includes all possible directed paths for each realization. The largest lattice size simulated is 1000×1000. The averaged probability distribution has been obtained by averaging Eq. (3) over 30 000 to 50 000 realizations of the disorder. We have carried out the calculation for several different temperatures in the range $\beta=1$–5 (where $\beta=1/kT$). The effect of temperature will be discussed later, but one expects the qualitative features of the model to be similar for different temperatures since in $1+1$ dimensions the scaling behavior is governed by a zero-temperature fixed point [7]. The simulations have been done on a Cray supercomputer, which allows for real numbers in the range $0.367\times 10^{-2465}<R<0.273\times 10^{2466}$. The results were checked for reproducibility on other machines.

In addition to the average probability $\langle P\rangle$, we have also calculated the averaged moments $\langle P^q(x,t)\rangle$ with $-1.9\le q\le 3$ and the histograms $\mathcal{P}(Y)$ with

$$Y=-\ln[P(x,t)] . \tag{7}$$

The histogram measures the number of realizations for which $-\ln(P)$ falls between Y and $Y+dY$. The averaged moments of the probability distribution and the histograms are related to each other by a Laplace transform:

$$\langle P^q(x,t,\beta)\rangle=\int_0^\infty e^{-qY}\mathcal{P}(Y;x,t,\beta)dY \tag{8a}$$

and its inverse

$$\mathcal{P}(Y;x,t,\beta)=\frac{1}{2\pi i}\int_{\delta-i\infty}^{\delta+i\infty} e^{qY}\langle P^q(x,t,\beta)\rangle dq . \tag{8b}$$

Loosely speaking, small-$|q|$ moments are primarily influenced by the region in which $\mathcal{P}(Y)$ has its maximum, i.e., by typical events, while large-$|q|$ moments are governed by the tail of $\mathcal{P}(Y)$, i.e., by rare events.

In Fig. 1, we have displayed some log-log plots of the

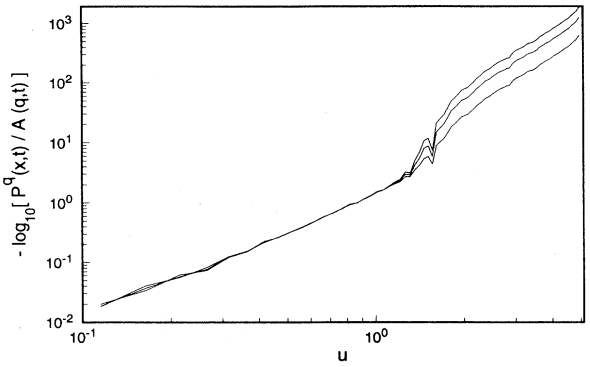

FIG. 1. A log-log plot of $-\log_{10}[\langle P^q(x,t)\rangle/A(q,t)]$ vs $u=|x|/t^{2/3}$, where $A(q,t)=\max[\langle P^q(x,t)\rangle]$ for $\beta=2.0$, $t=1000$, and $q=1.0$, 2.0 and 3.0 from bottom to top.

(normalized) moments of the probability distribution versus u, where the axes have been rescaled appropriately (see caption). One can clearly see the two regimes with different slopes (as noted above) and different q dependence. The slope changes from a value $y=2.1\pm 0.1$ in region 1 ($0.25\le u\le 1.2$) to $y=3.0\pm 0.1$ in region 2 ($2.0\le u\le 4.0$) with a transition region ($1.2\le u\le 2.0$). The q dependence is much more pronounced in region 2 for $1\le q\le 3$.

To aid in the analysis of the numerical results, we have introduced two functions $\tau(q;u,t,\beta)$ and $\hat{\tau}(q;u,t,\beta)$—the former more closely connected to the histograms, the latter more convenient for considering the scaling behavior. The first $\tau(q)$ is defined by the relation

$$\langle P^q(x,t,\beta)\rangle=\langle P(x,t,\beta)\rangle^{\tau(q;u,t,\beta)} \tag{9}$$

and satisfies $\tau(q=0)=0$ and $\tau(q=1)=1$. The second $\hat{\tau}$ is defined via

$$\langle P^q(x,t,\beta)\rangle=A(t,q,\beta)\exp\{-\hat{\tau}(q;u,t,\beta)u^{y}\} \tag{10}$$

in each of the scaling regimes (and y is the corresponding exponent in region 1 or 2). The functions τ and $\hat{\tau}$ differ by an overall multiplicative constant; in addition, the former includes the (weaker) q dependence of the coefficient A. In the following we will mainly consider τ and comment briefly on the behavior of $\hat{\tau}$.

To see the connection between $\tau(q)$ and the histograms, substitute Eq. (9) into Eq. (8b) to obtain

$$\mathcal{P}(Y)=\frac{1}{2\pi i}\int_{\delta-i\infty}^{\delta+i\infty} dq\, e^{-C\tau(q)+qY} , \tag{11}$$

where

$$C=-\ln\langle P(u,t,\beta)\rangle=\tfrac{2}{3}\ln(t)+\lambda u^{y}+\text{const} . \tag{12}$$

Note that C is large for large t (even for fixed u), and hence one can apply the method of steepest descent to the above integral. The integral is dominated by a value $q^*(\alpha)$ satisfying $\tau'(q^*)=Y/C\equiv\alpha$. One can thus express the distribution in the form

$$\mathcal{P}(Y)\approx\mathcal{N}\exp\{-Cf(Y/C)\} \tag{13}$$

with

$$f(\alpha)=\tau(q^*(\alpha))-q^*(\alpha)\alpha . \tag{14}$$

Hence, the function $\tau(q)$ describing the moments of P and the function $f(\alpha)$ characterizing the histograms are related by a Legendre transformation. Recalling the

definition of Y from Eq. (7), we obtain

$$P(u,t)=\exp\{-Y\}=\exp\{-\alpha C(u,t)\} \propto t^{2\alpha/3}\exp\{-\alpha\lambda u^{\nu}\}\ , \quad (15)$$

with the exponent α distributed among realizations according to

$$\mathcal{P}(\alpha)\approx C\mathcal{N}\exp\{-Cf(\alpha)\}\ . \quad (16)$$

Consider first the behavior in region 1. A study of τ in this region reveals that it has no (systematic) dependence on u and has a weak time dependence to be discussed below. We have calculated the function $f(\alpha)$ from Eq. (14) as the Legendre transform of $\tau(q)$. We have then used it to calculate $\mathcal{P}(Y)$ from Eq. (13), which is shown in Fig. 2 along with the histogram obtained directly from the simulation—the agreement is good.

The functions $\tau(q)$ and $f(\alpha)$ are displayed in Fig. 3 for $t=1000$ and $\beta=1$. The support of $f(\alpha)$ lies between $\alpha_{\min}$, which is slightly greater than zero and $\alpha_{\max}$. These values correspond to the derivatives of $\tau(q)$ for large $|q|$ and may be measured more precisely by simulating larger q values. The function $f(\alpha)$ can be fit to a polynomial by expanding it about its minimum $\alpha_{\rm typ}$:

$$f(\alpha)=a_2(\alpha-\alpha_{\rm typ})^2+a_3(\alpha-\alpha_{\rm typ})^3+a_4(\alpha-\alpha_{\rm typ})^4+\cdots , \quad (17)$$

where for $\beta=1$ we have found $\alpha_{\rm typ}=3.01$, $a_2=-1/2\tau''(0)=2.8\times10^{-2}$, $a_3=-5.3\times10^{-3}$, and $a_4=4.7\times10^{-3}$. The (small) nonquadratic terms introduce non-Gaussian corrections to the histograms $\mathcal{P}(Y)$. The value $\alpha_{\rm typ}=\tau'(0)$ provides, when substituted in Eq. (15), the value of $P(u,t)$ for a typical realization. Notice that $P_{\rm typ}(u,t)$ is smaller by several orders of magnitude from the value $\langle P(u,t)\rangle$ corresponding to $\alpha=1$. One can show that

$$\alpha_{\rm typ}=\langle \ln(P)\rangle/\ln\langle P\rangle\ , \quad (18)$$

and hence its deviation from 1 provides a measure for the lack of self-averaging of P. The large disparity between $P_{\rm typ}$ and $\langle P\rangle$ arises because, for some very rare configurations, P is significantly larger than $P_{\rm typ}$, and thus they shift the mean value considerably.

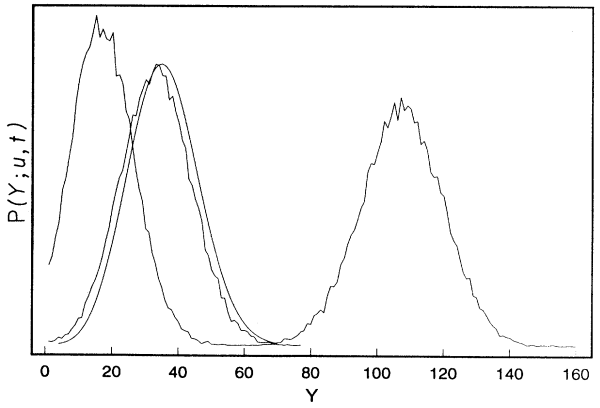

FIG. 2. Histograms $\mathcal{P}(Y;u,t)$ for $u=0.6$, 1.0, and 2.0 (from left to right) for $\beta=1.0$ and $t=1000$. The smooth curve is the fit for $u=1.0$ derived using Eq. (13).

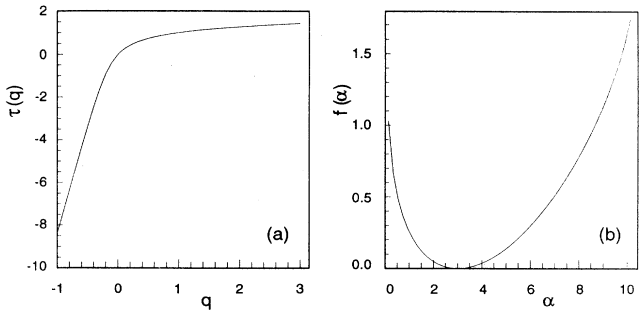

FIG. 3. (a) $\tau(q)$ in region 1 for $\beta=1$. (b) The corresponding $f(\alpha)$ (its Legendre transform).

Using $\hat{\tau}(q)$ instead of $\tau(q)$, one can repeat the steps outlined above; however, the results are somewhat less accurate since u^2 is not large enough in region 1 to justify the saddle-point approximation. We now comment on the temperature and time dependence of $\tau(q)$ and $f(\alpha)$. The quantity $C=-\ln\langle P\rangle$ has no apparent temperature dependence in region 1 for β's between 1 and 5. We have determined that the data in that temperature range nearly collapse if we plot the function $g(\alpha)=f_{\beta}(\beta^z\alpha)$ for $z\approx1$, where $f_{\beta}(\alpha)$ is the same as $f(\alpha)$ defined in Eq. (14), with the temperature dependence shown explicitly. This means in particular that $\alpha_{\rm typ}$ increases nearly linearly with β in that temperature range. It will be necessary to simulate lower temperatures in order to obtain the value of z in the limit of small T. As for the time dependence, we have discovered that $\tau'(0)=\alpha_{\rm typ}$ has a weak time dependence and behaves roughly like $t^{0.3}$ for large times. This is in agreement with the prediction of the toy model [4–6] (see below) that $\langle \ln(P)\rangle \propto -t^{1/3}u^2$.

Consider now region 2. In this region we have found that as u increases the function $\tau(q)$ becomes linear in q [$\tau(q)\approx q$]. The peak of its Legendre transform, $f(\alpha)$, migrates toward $\alpha=1$ [$=\tau'(0)$] and its width vanishes. Thus it can be said that $f(\alpha)$ becomes trivial. This implies in particular that for the large u, $\langle \ln(P)\rangle/\ln(\langle P\rangle)\to1$ as $u\to\infty$, and in this sense one might say that P becomes self-averaging.

Note, however, that the histograms of $Y=-\ln(P)$ do not necessarily become narrower as u increases, since $Y=C(u)\alpha$ and $C(u)$ grows with u. Only the ratio of the width to the position of the maximum of the histogram vanishes for large u. The numerical simulations suggest that the width of the Y histograms, initially growing, tends to saturate for large u, but an exact dependence on u cannot be established without simulating larger times.

Even for $u\approx1$, the range of α's originates mainly from fluctuations of $A(t)$, which is independent of u, as is indicated by the fact that $\hat{\tau}(q)$ defined in Eq. (10) is linear in q for all the range $u\geq2$. Thus for the entire range $u\geq2$, the exponential part of P, which behaves like $\sim\exp\{-\lambda_2u^3\}$, acquires a universal form that is independent of the realization.

The temperature dependence of λ_2 is nearly linear in β for large β, i.e., $\lambda_2=4.38\beta$. If this trend continues for

higher β's (the largest β we have considered is $\beta=5$), then it may suggest that the probability distribution evaluated strictly at $T=0$ will lack the u^3 region of the tail. However, we should note that some change in the scaling behavior for u slightly bigger than 1 has been observed in Ref. [7], where an effective exponent of $y=2.2$ is reported. To probe enough of the high-u region at $T=0$ and check whether it indeed crosses over to a different scaling behavior would require an enormous number of realizations.

We would like to point out that the value of u at which the scaling behavior of $\langle P(u,t)\rangle$ undergoes a change ($u_c \approx 1.2$) appears to coincide with the u value for which the tail of the histogram $\mathcal{P}(u,t;Y)$ pulls away from the $Y=0$ axis. (See Fig. 2.) Having a Y near zero implies having $P(u,t)$ near 1; therefore, $\langle P(u,t)\rangle$ changes its scaling behavior when $P(u,t)$ is significantly smaller than 1 for nearly all of the realizations generated.

The u^3 behavior we have observed in the tail has been predicted previously using the replica method. This formalism has led, using some approximations [4–6], to a mapping of the directed polymer problem into a related "toy" model with a Hamiltonian consisting of a quadratic piece $gx^2/2$ and a random potential $\phi(x)$, the slope of which is a Gaussian random variable [22]. Using this mapping, several authors have been led to a number of predictions, some in agreement with numerical simulations for directed polymers and some in apparent disagreement [4–7]. One of the predictions is that $\ln\langle P(u)\rangle \propto -u^3$ in the tail, as it is for the toy model [22]. The validity of this prediction for directed polymers has not been checked before, and our work shows that it agrees with the numerical measurements. There does not seem to be a general criterion at this time to distinguish which of the predictions of the toy model is accurate.

To conclude, we have investigated the behavior of the probability distribution for directed polymers in random media and have discovered two distinct scaling regimes in terms of the scaling variable $x/t^{2/3}$. The distribution of scaling exponents for the probability distribution among various realizations of the disorder is governed by a convex universal function $f(\alpha)$, which is related via a Legendre transformation to the function $\tau(q)$ characterizing the averaged qth moment of the probability. The function $f(\alpha)$ is also related to the shape of the histograms of $-\ln(P)$ among different realizations. In the inner scaling region, $f(\alpha)$ is broad, whereas in the outer scaling region its width shrinks to zero for large u, implying a realization-independent (self-averaging) form of $\langle P\rangle$ in this limit.

This work was supported by the National Science Foundation under Grant No. DMR-9016907. We also thank the Pittsburgh Supercomputer Center for computing time allocation under Grant No. PHY910027P.

[1] D. A. Huse and C. L. Henley, Phys. Rev. Lett. **54**, 2708 (1985).

[2] M. Kardar, Phys. Rev. Lett. **55**, 2923 (1985); Nucl. Phys. B **290**, 582 (1987).

[3] D. A. Huse C. L. Henley, and D. S. Fisher, Phys. Rev. Lett. **55**, 2924 (1985).

[4] G. Parisi, J. Phys. (Paris) **51**, 1595 (1990).

[5] M. Mézard, J. Phys. (Paris) **51**, 1831 (1990).

[6] J. P. Bouchaud and H. Orland, J. Stat. Phys. **61**, 877 (1990).

[7] T. Halpin-Healy, Phys. Rev. A **44**, R3415 (1991).

[8] D. S. Fisher and D. A. Huse, Phys. Rev. B **43**, 10728 (1991).

[9] J. M. Kim, M. A. Moore, and A. J. Bray, Phys. Rev. A **44**, 2345 (1991); J. Krug, P. Meakin, and T. Halpin-Healy, *ibid.* **45**, 638 (1992).

[10] C. Poirier, M. Ammi, D. Bideau, and J. P. Troadec, Phys. Rev. Lett. **68**, 216 (1992).

[11] M. Mézard and G. Parisi, J. Phys. (France) I **1**, 809 (1991); and J. Phys. A **23**, L1229 (1990).

[12] M. Kardar, G. Parisi, and Y. C. Zhang, Phys. Rev. Lett. **56**, 889 (1986).

[13] T. C. Halsey, M. H. Jensen, L. P. Kadanoff, I. Procaccia, and B. I. Shraiman, Phys. Rev. A **33**, 1141 (1986).

[14] B. B. Mandelbrot, J. Fluid Mech. **62**, 331 (1974); U. Frisch and G. Parisi, in *Turbulence and Predictability in Geophysical Fluid Dynamics and Climate Dynamics,* Proceedings of the International School of Physics "Enrico Fermi," Course LXXXVIII, edited by M. Ghil *et al.* (North-Holland, New York, 1985).

[15] P. Meakin, A. Coniglio, H. E. Stanley, and T. A. Witten, Phys. Rev. A **34**, 3325 (1986); M. E. Cates and T. A. Witten, Phys. Rev. Lett. **56**, 2497 (1987).

[16] F. Wegner, Z. Phys. B **36**, 209 (1980); C. Castellani and L. Peliti, J. Phys. A **19**, L429 (1986).

[17] Y. Park, A. B. Harris, and T. C. Lubensky, Phys. Rev. B **35**, 5048 (1987).

[18] *Fractals and Disordered Systems,* edited by A. Bunde and S. Havlin (Springer-Verlag, Berlin, 1991).

[19] A. W. W. Ludwig, Nucl. Phys. B **330**, 639 (1990).

[20] M. Araujo, S. Havlin, and H. E. Stanley, Phys. Rev. A **44**, 6913 (1991).

[21] In the actual simulations, we have eliminated the intervening zeros, which has the effect of scaling x down by a factor of 2.

[22] J. Villain, B. Séméria, F. Lançon, and L. Billard, J. Phys. C **16**, 6153 (1983); and U. Schulz, J. Villain, E. Brézin, and H. Orland, J. Stat. Phys. **51**, 1 (1988).